

# Kinetic and Thermodynamic Study of the Interactions of Nickel(II) with Nicotinamide Adenine Dinucleotide and Nicotinamide Adenine Dinucleotide Phosphate

Joseph P. Bidwell<sup>†</sup> and John E. Stuehr\*

Received May 12, 1989

The equilibria and kinetics of Ni(II) interactions with the two pyridine coenzymes NAD and NADP were investigated by the temperature-jump relaxation technique. Three relaxation times for each system were detected, of which the two slower were characterized in detail as a function of metal ion and ligand concentrations and pH. The two slow times,  $\tau_2$  and  $\tau_3$ , were in the  $10^{-3}$  and  $10^{-1}$  s time regions, respectively. Both times for NAD were only slightly concentration and pH dependent; those for NADP were strongly pH dependent. These results were found to be consistent with a mechanism involving sequential formation of several different 1:1 metal ion complexes, including those in which the various ring systems participated with phosphate bonding. For NADP, a parallel series of steps involving the phosphate-protonated coenzyme was also present. Rate constants were compared to those for corresponding steps in simpler nucleotide and phosphate systems. A major conclusion from this study was that the kinetic behavior of the simpler systems was retained even in the largest metal ion complexes. We call this behavior "kinetic integrity".

## Introduction

Our laboratory has carried out a series of kinetic studies of divalent metal ion interactions with various phosphates and nucleotides<sup>1</sup> (e.g. ribose phosphate, 2',3'- and 5'-AMP, and FMN).<sup>2-4</sup> Recently, we turned our attention to the interactions of Ni(II) with the dinucleotide FAD,<sup>4</sup> a coenzyme which is structurally a combination of the mononucleotides FMN and 5'-AMP (Figure 1). For that system, we found four relaxation processes, corresponding to metal ion interactions with the phosphate moieties and the individual ring systems. One of the main conclusions of that study was that the component parts of the dinucleotide retained their individual kinetic properties. The Ni(II)-dinucleotide system could be interpreted as a Ni-phosphate interaction followed by a series of interactions with the ring systems, each such interaction having rate and binding constants characteristic of the simpler systems (phosphate, AMP base, etc.) modified somewhat by the dinucleotide's tendency to stack in aqueous solutions.

The Ni-FAD results are significant because they suggest that kinetic and thermodynamic data from the metal-*mononucleotide* and *-dinucleotide* systems also provide information about metal-*polynucleotide* interactions. This is particularly noteworthy in light of recent evidence that low concentrations of divalent nickel stabilize the Z form of DNA and that these complexes may play a role in transcription.<sup>5</sup>

To test the hypothesis that the complex interaction of a metal-dinucleotide system is a combination of the metal constituent mononucleotide mechanisms, we now turn our attention to the pyridine dinucleotides NAD and NADP. The cofactor NAD (Figure 1) is structurally similar to FAD except that it is a combination of 5'-AMP and nicotinamide mononucleotide (NMN). The phosphate derivative, NADP, can be considered to be a composite of three mononucleotides: NMN and 2'- and 5'-AMP. Both pyridine dinucleotides, like FAD, assume folded conformations in aqueous solution,<sup>6-8</sup> however, the positively charged nicotinamide ring presents an interesting variation with respect to metal ion interactions.

The biological importance of nickel is no longer a matter of conjecture, since biochemical studies have shown it to be a cofactor for enzymic systems in methanogenic bacteria.<sup>9,10</sup> In addition, recent work suggests that nickel is involved in eukaryotic transcription.<sup>5</sup>

NAD and NADP are essential coenzymes for catalytic activity of the alcohol dehydrogenases, a family of enzymes (many containing zinc) involved in alcohol fermentation and implicated in ethanol metabolism.<sup>11,12</sup> Despite extensive studies<sup>12-16</sup> on structural aspects of cofactor-protein interactions, information on metal-coenzyme complexes is limited to the binding constants

**Table I.** pK Values and Ni(II) Stability Constants for Pyridine Coenzymes<sup>a</sup>

	NMN	NAD	NADP
pK <sub>a1</sub>		3.72	3.87
pK <sub>a2</sub>	5.71		6.06
log K <sub>ML</sub>	1.54	1.90 <sup>b</sup>	2.52
log K <sub>MHL</sub>			1.53

<sup>a</sup> At 15 °C and *I* = 0.1 M (KNO<sub>3</sub>). <sup>b</sup> Estimated; see text.

for Zn and Cu with NAD.<sup>17,18</sup> The fundamental interactions between metal ions and the pyridine dinucleotides remain to be kinetically characterized. The purpose of this paper is 2-fold: to provide results of the first kinetic and thermodynamic study of the metal-pyridine coenzyme interactions and to test the hypothesis of "kinetic integrity" through a detailed comparison of rate and thermodynamic constants for the nickel-dinucleotide systems Ni-FAD, Ni-NAD, and Ni-NADP with those for the nickel constituent mononucleotide complexes.

## Experimental Section

**Materials.** The sodium salt of  $\beta$ -NADP and the free acids of  $\beta$ -NAD

- (1) Frey, C. M.; Stuehr, J. E. In *Metal Ions in Biological Systems*; Sigel, H., Ed.; M. Dekker: New York, 1974; Vol. I, pp 51-116.
- (2) Thomas, J. C.; Frey, C. M.; Stuehr, J. E. *Inorg. Chem.* **1980**, *19*, 501-504.
- (3) Thomas, J. C.; Frey, C. M.; Stuehr, J. E. *Inorg. Chem.* **1980**, *19*, 505-510.
- (4) Bidwell, J.; Thomas, J.; Stuehr, J. E. *J. Am. Chem. Soc.* **1986**, *108*, 820-825.
- (5) Adams, S.; Bourtayre, P.; Liquier, J.; Taillandier, E. *Nucleic Acids Res.* **1986**, *14*, 3501-3513.
- (6) Kainosho, M.; Kyogoku, J. *Biochemistry* **1972**, *11*, 741-752.
- (7) Hamill, D. W.; Pugmire, R. J.; Grant, D. M. *J. Am. Chem. Soc.* **1974**, *96*, 2885-2887.
- (8) Walter, C.; Hollis, D.; Brown, B.; McDonald, G. *Biochemistry* **1972**, *11*, 1920-1930.
- (9) Eleafson, W. L.; Whitman, W. B.; Wolfe, R. S. *Proc. Natl. Acad. Sci. U.S.A.* **1982**, *79*, 3707-3710.
- (10) Hausinger, R. P.; Orme-Johnson, W. H.; Walsh, C. *Biochemistry* **1984**, *23*, 801-804.
- (11) Walsh, C. *Enzymatic Reaction Mechanisms*; W. H. Freeman and Co.: San Francisco, 1979; pp 322-330.
- (12) Bränden, C.-I.; Jörnvall, H.; Eklund, H.; Furugren, B. In *The Enzymes*, 3rd ed.; Boyer, P. D., Ed.; Academic Press: New York, 1975; Vol. XI, pp 103-190.
- (13) Klinman, J. P. *CRC Crit. Rev. Biochem.* **1981**, *10*, 39-78.
- (14) Maret, W.; Andersson, I.; Dietrich, H.; Schneider-Bernlöhr, H.; Einarsson, R.; Zeppezauer, M. *Eur. J. Biochem.* **1979**, *98*, 501-512.
- (15) Eklund, H.; Samama, J.-P.; Jones, T. A. *Biochemistry* **1984**, *23*, 5982-5996.
- (16) Schneider, G.; Eklund, H.; Zeppezauer, E. C.; Zeppezauer, M. *EMBO J.* **1983**, *2*, 685-689.
- (17) Weitzel, G.; Spehr, T. *Hoppe-Seyler's Z. Physiol. Chem.* **1958**, *313*, 212-226.
- (18) Wallenfels, K.; Sund, H. *Biochem. Z.* **1957**, *329*, 41-47.

<sup>†</sup> Present address: Endocrine Research Unit, The Mayo Clinic, Rochester, MN 55905.

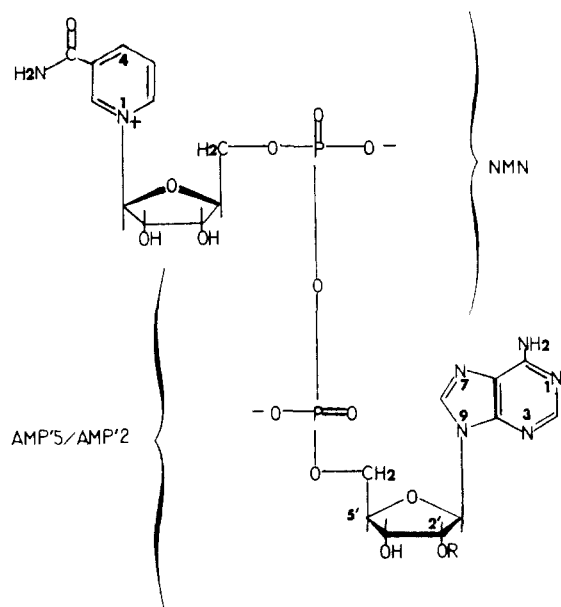


**Figure 1.** Structure of NAD and its relation to other nucleotides. NADP is formed by converting the R on the 2' ribose to a phosphate group.

and  $\beta$ -NMN of the highest purity were obtained from Sigma Chemical Co. Solutions were prepared daily in 0.1 M KNO<sub>3</sub> and passed through a 0.45- $\mu$ m Millipore filter. All samples were protected from light. The Ni(II) stock solutions were prepared from reagent grade nickel nitrate (Baker) and standardized spectrophotometrically.<sup>19</sup>

**Methods: Equilibrium Constants and Kinetics.** The  $pK_a$ 's and stability constants were obtained at 15 °C and  $I = 0.1$  M (KNO<sub>3</sub>) by potentiometric titration.<sup>20,21</sup> The kinetic experiments were carried out by temperature-jump spectroscopy, as previously described.<sup>4</sup> The relaxation effects were monitored either via near-UV spectral measurements of the metal–dinucleotide solution (300 nm) or by coupling the reaction to a pH indicator, i.e. chlorophenol red (CPR) or bromophenol blue (BPB) with detection wavelengths of 575 or 592 nm, respectively. The concentrations of ligand and metal ion ranged from 1 to 20 mM. The ligand:metal ratio was near unity in most cases. Blanks containing only ligand and indicator or metal ion and indicator were tested to ensure that the observed relaxation spectra resulted from the metal–ligand interactions.

The relaxation data were collected and stored on a Biomation transient recorder, the output of which was displayed on an oscilloscope screen. The relaxation times were obtained either from Polaroid photographs of the relaxation traces or from computer analysis of the digitized data.<sup>22</sup> Precision of replicate experiments was typically  $\pm 5$ –10%.

## Results

**Ionization and Binding Constants.** The  $pK_a$  and Ni(II) stability constant values for NAD, NADP, and NMN, as determined by potentiometric titration, are listed in Table I. There are three ionizable protons on NAD: two on the phosphate bridge, each with a value of approximately 2 (not characterized), and a third on the adenine ring (N1,  $pK_{a3} = 3.72$ ). The addition of the terminal phosphate at the 2'-ribose position in NADP results in two more ionizable sites. The primary and secondary proton ionizations have  $pK_a$  values of  $\sim 2$  and 6.06, respectively.

As was found for FAD,<sup>4</sup> the shift in the pH titration curve or UV-difference spectra for NAD upon the addition of Ni(II) was too small to allow an accurate determination of the binding constant.

**Kinetics.** The Ni–NAD and –NADP systems each showed three relaxation times, the two slower of which could be completely characterized in terms of their concentration and pH dependences. A very fast relaxation effect ( $\tau_1$ ) has an amplitude too small for accurate characterization; this effect corresponds to the Ni–phosphate interactions, as also seen<sup>1–4</sup> in the other metal–nucleotide

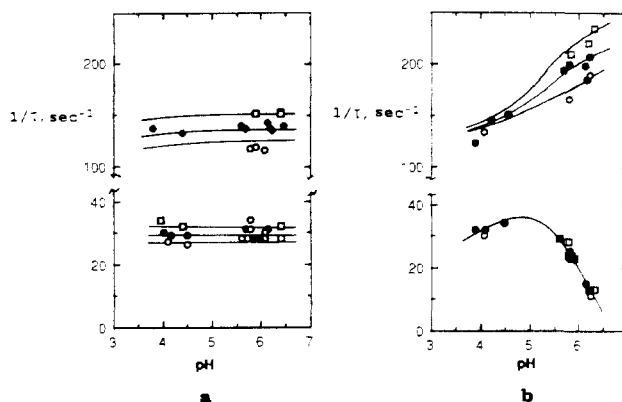
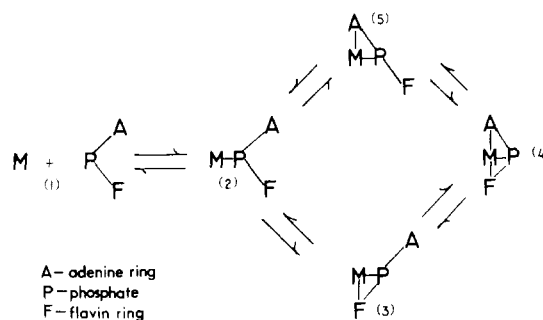


**Figure 2.** Concentration and pH dependences of the relaxation times  $\tau_2$  (top) and  $\tau_3$  (bottom) in (a) Ni–NAD and (b) Ni–NADP. Lines are theoretical curves predicted for Scheme II.  $[M]_0 = [L]_0$ :  $\square$ , 20 mM;  $\bullet$ , 10 mM;  $\circ$ , 5 mM.

## Scheme I



systems. The relaxation profiles for  $\tau_2$  and  $\tau_3$  for the two systems were similar in some respects and different in others. The faster effect ( $\tau_2$ ) for both systems was in the 5-ms time region; the slower was in the 35-ms region (see Table II, supplementary material). Dilute Ni–NAD and Ni–NADP solutions are very slightly colored. We found that the slowest relaxation effects could be followed either with indicator (575 or 592 nm) or without indicator by monitoring in the near-UV region ( $\sim 300$  nm). The faster effect however could be monitored only with a pH indicator.

The faster of the two observed relaxation rates ( $\tau_2^{-1}$ ) was slightly concentration dependent (Figure 2). For Ni–NAD, the values ranged from 116 to 152 s<sup>-1</sup> over the concentration range 0.001–0.02 M. The corresponding values for Ni–NADP varied from 155 to 265 s<sup>-1</sup>. On the other hand, the slower relaxation rates for both systems ( $\tau_3^{-1}$ ) were not only concentration independent but nearly identical numerically with that found earlier for the Ni–FAD system.<sup>4</sup>

The pH dependences of the two relaxation times for the two systems were strikingly different. For Ni–NAD, both relaxation times were, within experimental error, very nearly pH independent (Table II and Figure 2a). For Ni–NADP, on the other hand, both relaxation times were pH dependent: over the pH range 3.9–6.2,  $\tau_2^{-1}$  varied from 124 to 176 s<sup>-1</sup> and  $\tau_3^{-1}$  from 32 to 13 s<sup>-1</sup>. Figure 2 shows the pH dependence of the relaxation rates at several different concentrations for both systems.

**Mechanism.** The similarities in the relaxation behavior of the two systems to that found<sup>4</sup> for the Ni–FAD system suggest that the mechanisms are similar. The mechanism determined for Ni–FAD is shown<sup>37</sup> as Scheme I, where P, A, and F correspond to the phosphate, adenine, and flavin moieties of the dinucleotide and the solid lines represent direct bonding between the groups as indicated.

NADP differs kinetically from FAD in two ways. The species corresponding to 3 in Scheme I apparently does not exist for NADP, and the additional secondary phosphate group generates a parallel sequence of *protonated* reaction pathways. The mechanism shown as Scheme II is consistent with all the experimental results for the Ni–NAD and –NADP systems. In this

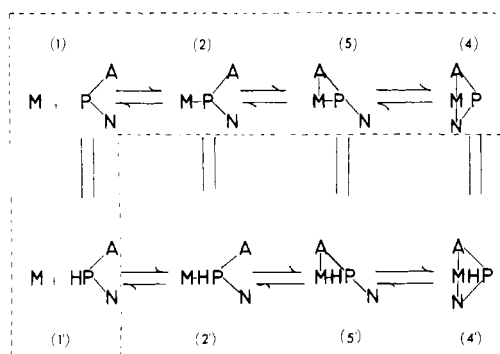
(19) Bidwell, J. P. Ph.D. Thesis. Case Western Reserve University, 1983.

(20) Briggs, T. N.; Stuehr, J. E. *Anal. Chem.* **1974**, *46*, 1517–1521.

(21) Briggs, T. N.; Stuehr, J. E. *Anal. Chem.* **1975**, *47*, 1916–1920.

(22) Lipson, K. E. Ph.D. Thesis. Case Western Reserve University, 1982.

Scheme II



scheme, the symbols P, N, and A represent the phosphate moieties, the pyridine ring, and the adenine ring, respectively, of the coenzymes NAD and NADP. The slow complexation steps are indicated by arrows; the rapid proton-transfer equilibria, by = signs. The bottom row includes complexes protonated on the secondary phosphate of NADP. That part of the mechanism which applies to NAD, which does not have the extra protonation site present in NADP, is outlined (---) and designated as Scheme IIa.

We propose that the metal ion initially binds to the phosphate moiety via step 1–2, i.e., to the bridge phosphates and both the bridge terminal phosphate groups in NAD and NADP, respectively. This results in the relaxation time  $\tau_1$ . The bound nickel then interacts ( $\tau_2$ ) with the adenine ring of the pyridine dinucleotide,<sup>23</sup> step 2–5, as it does with the flavin coenzyme. Finally, the slowest step, corresponding to  $\tau_3$ , is 5–4, in which both bases interact with the metal ion. The dinucleotide's tendency to form a folded conformation<sup>7,8</sup> allows the nickel ion and the positively charged nicotinamide ring to come into close association.

**Ni–NAD.** As shown in Scheme IIa,  $\text{Ni}^{2+}$  forms three complexes with NAD involving sequential interactions with the phosphate moiety, the phosphate plus adenine ring, and the phosphate plus a simultaneous interaction with both the nicotinamide and adenine rings (the foldover complex). There are three independent concentration variables in Scheme IIa, which result in the three relaxation times given by the  $3 \times 3$  determinant

$$\begin{vmatrix} a_{11} - \lambda & a_{12} & a_{13} \\ a_{21} & a_{22} - \lambda & a_{23} \\ a_{31} & a_{32} & a_{33} - \lambda \end{vmatrix} = 0 \quad (1)$$

where  $\lambda_i$  are the roots of the determinant and are equal to  $-1/\tau_i$ .

The  $a_{ij}$  terms are coefficients of the three independent concentration variables. If one chooses them to be  $C_1$ ,  $C_4$ , and  $C_5$  in Scheme IIa, the explicit coefficients are

$$\begin{aligned} a_{11} &= -(k_{12}[\text{M}]/(1 + \beta)) + [L] + k_{21} & a_{12} &= -k_{21} & a_{13} &= -k_{21} \\ a_{21} &= -k_{25} & a_{22} &= -(k_{25} + k_{52} + k_{54}) & a_{23} &= -k_{25} + k_{45} \\ a_{31} &= 0 & a_{32} &= k_{54} & a_{33} &= -k_{45} \end{aligned}$$

where  $\beta = [\text{H}]/[K_a + [\text{L}]/(1 + \alpha)]$ ,  $\alpha = [\text{In}]/(K_{\text{In}} + [\text{H}])$ , all concentrations are equilibrium values, and  $K_a$  and  $K_{\text{In}}$  are the ionization constants for the nucleotide and indicator, respectively.

There are three independent rate constants and three unknown equilibrium constants in Scheme IIa. The rate constant  $k_{12}$  was taken to be  $2 \times 10^5 \text{ M}^{-1} \text{ s}^{-1}$ , primarily on the basis of previous work for the Ni–phosphate interaction;<sup>1–4</sup> as noted above, we did not characterize the corresponding relaxation time in the present work. The remaining constants were determined by a nonlinear regression technique<sup>24</sup> in which the constants were systematically varied so

as to give the best agreement between the experiment  $\tau_i^{-1}$  and the predicted  $\lambda_i$ . Statistical analysis showed that the Ni–NAD mechanism was insensitive to the value of  $K_{\text{ML}}$  within the limits of  $30 < K_{\text{ML}} < 250$ . This constant was only weakly coupled to all other constants of the scheme; therefore, a reasonable value ( $K_{\text{ML}} = 80$ ) was chosen on the basis of our statistical analysis and the few available literature values for other metal ions.<sup>17,18</sup> A complete list of relaxation data for the Ni–NAD system is given in Table II. Part of the data is shown in Figure 2 and compared with the behavior predicted by eq 1.

**Ni–NADP.** As noted earlier, the presence of another phosphate group in this system, with a rate expression for secondary phosphate ionization of about 6.1, results in a parallel, pH-dependent pathway. This is shown in the mechanism given as Scheme II. The presence of the protonated pathway leads to a considerably more complicated mathematical formulation, but there are still only three relaxation times. The details of the mathematical analysis of the parallel rate expressions and the resulting  $3 \times 3$  determinant are given elsewhere.<sup>19</sup>

Scheme II has six independent rate and four independent equilibrium constants. The other equilibrium constants are either known or are fixed by identities relating them to the other constants. As for the Ni–NAD system, we did not characterize the phosphate interactions; the rate constants,  $k_{12}$  and  $k'_{12}$  were set equal to those for analogous interactions in other phosphate-containing systems.<sup>1–4</sup> The least-squares fitting procedure was generally sensitive to all the remaining independent rate constants in Scheme II. Table II compares the experimental values,  $\tau_2^{-1}$  and  $\tau_3^{-1}$ , with the predicted  $\lambda_2$  and  $\lambda_3$ . Some of the data are shown graphically in Figure 2 as a function of concentration and pH.

## Discussion

Table III is a compilation of the best-fit rate and equilibrium constants for this study along with the constants for Ni–FAD and the mononucleotides that constitute these pyridine and flavin coenzymes. The following discussion is largely based on comparisons from this table.

**Phosphate Interaction (Steps 1–2 and 1'–2').** The initial metal–cofactor interactions, as represented by the binding and forward rate constants ( $K_{12}$  and  $k_{12}$ , respectively) for the Ni–(II)–phosphate complex, are nearly identical for all the mononucleotides ( $K_{12} = 80 \text{ M}^{-1}$ ,  $k_{12} = 2.0 \times 10^5 \text{ M}^{-1} \text{ s}^{-1}$ ). The smaller value for the Ni–NAD and Ni–FAD binding constants ( $\sim 20 \text{ M}^{-1}$ ) is consistent with the weaker metal interaction with the bridge phosphates. The relatively large value of  $120 \text{ M}^{-1}$  for Ni–NADP is a result of the metal's binding to both the bridge and 2'-phosphate groups. The rate constants  $k_{12}$  and  $k'_{12}$  for the Ni–NAD/NADP reactions could not be accurately determined in this study. Nevertheless, the values of these rate constants appear to be virtually constant for the wide variety of Ni(II)–nucleotide systems we have previously characterized.<sup>1–4</sup>

**Phosphate–Adenine Ring Interaction (Step 2–5).** We see no evidence for isolated metal ion–base ring interactions. It is only upon binding to the phosphate groups of these cofactors that nickel can interact with the ring moieties. The binding constants for the simultaneous phosphate-bound metal–adenine ring interaction,  $K_{25}$ , are nearly identical for the Ni–FAD, Ni–NAD, and Ni–AMP systems (3, 3, and  $4 \text{ M}^{-1}$ , respectively). The strained interaction among the metal, the 2'-phosphate group, and the adenine base ring is reflected in the reduced values of  $K_{25}$  for Ni–NADP and Ni–2'-AMP ( $1.5$  and  $0.67 \text{ M}^{-1}$ , respectively). Similarly, the rate constant,  $k_{25}$ , is significantly smaller for Ni–2'-AMP than for Ni–5'-AMP. This rate constant is nearly the same for all the dinucleotides ( $200$ – $300 \text{ s}^{-1}$ ) and is some 2–4-fold smaller than that for the constituent mononucleotide system Ni–5'-AMP ( $1510 \text{ s}^{-1}$ ). This may be the result of the necessity for the phosphate-bound nickel to disrupt the folded conformation or ring-stacking interaction of the dinucleotide before the individual complexation with the adenine base ring can occur. A similar reduction in the rate

(23) The phosphate-bound metal ion does not directly interact with the positively charged nicotinamide ring, step 2–3, analogous to the Ni–isalloxazine base interaction in the FAD mechanism,<sup>4</sup> Scheme I.

(24) Feltch, S. Ph.D. Thesis. Case Western Reserve University, 1980.

**Table III.** Rate and Equilibrium Constants for the Interaction of Ni(II) with Mono- and Dinucleotides<sup>a</sup>

	Ni-FAD <sup>b</sup>	Ni-NAD <sup>c</sup>	Ni-NADP <sup>c</sup>	Ni-FMN <sup>b</sup>	Ni-5'-AMP <sup>d</sup>	Ni-2'-AMP <sup>d</sup>	Ni-RiPO <sub>4</sub> <sup>e</sup>
Phosphate Complexes							
$K_{12}$ , M <sup>-1</sup>	20 ± 5	15 ± 5	120 ± 5	72.6	80	90	80
$K'_{12}$ , M <sup>-1</sup>			15 ± 5	5	2	3.3	5
$10^{-3}k_{12}$ , M <sup>-1</sup> s <sup>-1</sup>	2.0 ± 0.7	2.0	2.0	1.47	2.3	1.8	1.4
$10^{-4}k'_{12}$ , M <sup>-1</sup> s <sup>-1</sup>			2.0	2.46	2.0	3.5	3.3
Phosphate-Adenine Ring Complexes							
$K_{25}$	3.0 ± 0.5	3 ± 1	1.5 ± 0.2		4	0.67	
$K'_{25}$			0.7 ± 0.1		6.5	0.5	
$k_{25}$ , s <sup>-1</sup>	550 ± 200	230 ± 100	200 ± 50		1510	175	
$k'_{25}$ , s <sup>-1</sup>			40 ± 10		1670	440	
Phosphate-Isoalloxazine or Nicotinamide Complexes							
$K_{23}$	0.62 ± 0.1			0.62			
$k_{23}$ , s <sup>-1</sup>	130 ± 20			246			
$k'_{23}$ , s <sup>-1</sup>							
Nicotinamide-Adenine-Isoalloxazine Nicotinamide Complexes							
$K_{34}$	18.2						
$K_{54}$	2.6	0.4	0.17				
$K'_{54}$			0.81				
$k_{54}$ , s <sup>-1</sup>	60 ± 30	25 ± 10	1 ± 1				
$k'_{54}$ , s <sup>-1</sup>			50 ± 10				
$k_{34}$ , s <sup>-1</sup>	30 ± 30						

<sup>a</sup> At 15 °C and  $I = 0.1$  M (KNO<sub>3</sub>). <sup>b</sup> Reference 4. <sup>c</sup> This work. <sup>d</sup> Reference 3. <sup>e</sup> Reference 2.

constant for the individual ring interaction with the flavin base is seen when one compares  $k_{23}$  for Ni-FMN and Ni-FAD.

**Phosphate-Adenine-Pyridine/Flavin Interaction (Step 5-4), the Foldover Complex.** In the Ni-NAD/NADP mechanism discussed above, we proposed that a foldover complex is formed in which the Ni(II) ion interacts with both nucleotide base rings, similar to that proposed for the Ni-FAD system.<sup>4</sup> The favored folded conformation of the dinucleotides<sup>6-8</sup> along with the basic CONH<sub>2</sub> group of the pyridine ring apparently compensates for the charge repulsion of the pyridine moiety and the Ni(II) ion. This type of "encouraged" interaction has been documented<sup>25</sup> in metal ion-polynucleotide interactions.

The interaction of the dinucleotide foldover complex is much weaker in the Ni(II) pyridine systems than in the Ni-FAD systems: the value of  $K_{54}$  is nearly an order of magnitude smaller. Again, we attribute this to the weak interaction between the metal ion and the positively charged nicotinamide ring. Nevertheless, the forward rate constants for the formation of this metal ring-stacked complex,  $k_{54}$ , are nearly identical for Ni-NAD and Ni-NADP. As previously mentioned, the protonation of the 2'-phosphate of NADP imparts NAD-like character to some aspects of this coenzyme's interactions with nickel, as shown by the values of  $k'_{54}$  and  $K'_{12}$ .

**Relevance to Enzyme Systems.** Until now, a detailed picture of the metal-pyridine coenzyme interaction has not appeared in the literature. This information represents a necessary complement to investigations concerned with the structural and mechanistic features of the alcohol dehydrogenases.<sup>12-16</sup> The oxidized form of these pyridine dinucleotides has a number of potential metal binding sites despite the presence of the positively charged ring, and even this moiety can be forced into interaction with the metal if the dinucleotide is free to bend. The fact that the metal ion may not be required for coenzyme binding on some proteins<sup>15,16</sup> does not preclude a strong interaction between these two cofactors. In this context, we might ask not only whether there is a direct interaction in the enzymic complex but also how one could be prevented in the close confines of the active site.

In a broader context, our studies demonstrate that the constituent mononucleotides of the dinucleotide coenzyme maintain their "kinetic integrity" with respect to metal ion interactions. The rate and equilibrium constants for the metal-dinucleotide schemes reflect values for the individual steps characterized for the metal-mononucleotide systems. They are, however, somewhat modified by the necessity for the metal ion to disrupt the folded

conformation of the dinucleotide before the individualized base ring complexation can occur.

The characterization of the phenomenon of kinetic integrity, along with the compilation of rate and thermodynamic constants for the nickel-mononucleotide and -dinucleotide systems (Table III), may provide a "key" for understanding metal-polynucleotide interactions. Such studies, for example, may provide additional insights into the nickel-induced B to Z transition in DNA.<sup>5,26</sup> The B DNA (right-handed helix) is the most prevalent conformational form in biological systems.<sup>27</sup> The Z form is a left-handed, antiparallel double helix that zigzags with a *dinucleotide* repeating unit as a consequence of the alternation of the syn and anti conformations at the guanines and cytosines, respectively.<sup>28,29</sup> Through the use of selectively deuterated polynucleotides, IR spectroscopy indicates that Ni(II) interacts directly with the N7 of the purine bases, accounting, at least partly, for the stabilization of the syn conformation.<sup>26</sup> The data compiled in Table III of this study clearly show that the Ni(II)-adenine base interaction is strong and persistent in a variety of chemical environments. Our work also indicates that nickel binds with both terminal and nonterminal phosphates. This information is important because such interactions at the phosphate-deoxyribose bridges of DNA may play a part in favoring the Z form. The ordering of the water shell around the A-T base pairs, because of the presence of Ni(II), may also provide additional stabilization to the Z form.<sup>26</sup> The role of Z DNA in vivo is a subject of considerable controversy, but it has been suggested that this conformational form,<sup>27</sup> along with nickel,<sup>26</sup> may be involved in the regulation of transcription. Speculation concerning this metal's role in biological systems has intensified since its recent emergence as a required element for a number of methanogenic bacteria.<sup>29-32</sup> In any case, metal ions can act as cofactors for enzymes that use DNA as a substrate, such as RNA polymerase III or binding proteins, e.g. transcription factor IIIA (TFIIIA).<sup>33-35</sup> Not only have transition-metal

(26) Taillandier, E.; Tabouray, J. A.; Adams, S.; Liquier, J. *Biochemistry* **1984**, *23*, 5703-5706.

(27) Rich, A. *Cold Spring Harbor Symp. Quant. Biol.* **1982**, *1*, 1-12.

(28) Barton, J. K. *Science* **1986**, *233*, 727-734.

(29) Friedrich, B.; Heine, E.; Finck, A.; Friedrich, G. G. *J. Bacteriol.* **1981**, *145*, 1144-1149.

(30) Bartha, R.; Ordal, E. J. *J. Bacteriol.* **1965**, *89*, 1015-1019.

(31) Kiekert, G.; Thauer, R. K. *FEMS Microbiol. Lett.* **1980**, *7*, 187-189.

(32) Drake, H. L.; Hu, S.-L.; Wood, H. G. *J. Biol. Chem.* **1980**, *255*, 7174-7180.

(33) Mildvan, A. S.; Loeb, L. A. *CRC Crit. Rev. Biochem.* **1979**, *6*, 219-244.

(34) Miller, J.; McLachlan, A. D.; Klug, A. *EMBO J.* **1985**, *4*, 1609-1614.

(35) Parraga, B.; Horvath, S. J.; Eisen, A.; Taylor, W. E.; Hood, L.; Yound, E. T.; Klevit, R. E. *Science* **1988**, *241*, 1489-1492.

complexes been used as molecular probes to characterize DNA polymorphism, but they have also been central in the development of synthetic restriction enzymes.<sup>36</sup> Interest in the fundamental interactions between metal ions and nucleotides is enhanced by

the growing body of evidence from molecular studies that such interactions may play a major role in genetic expression.

**Acknowledgment.** This research was supported by the National Institutes of Health in the form of a research grant to J.E.S. (GM 13,116). J.P.B. gratefully acknowledges support from the B. F. Goodrich Corp. in the form of a research fellowship.

**Supplementary Material Available:** Table II, listing kinetic data for the interaction of Ni(II) with NAD and NADP (5 pages). Ordering information is given on any current masthead page.

(36) Barton, J. K. *Chem. Eng. News* **1988**, *66*, 30-42.

(37) We have included the mechanism for the Ni-FAD system to provide a comparison and to minimize confusion when individual steps in the metal-mono-nucleotide and -dinucleotide systems, are compared. A single numbering system is used throughout.

Contribution from the NMR Section, Department of Radiology, Massachusetts General Hospital and Harvard Medical School, Boston, Massachusetts 02114

## Structure-Affinity Relationships in the Binding of Unsubstituted Iron Phenolate Complexes to Human Serum Albumin. Molecular Structure of Iron(III) *N,N'*-Bis(2-hydroxybenzyl)ethylenediamine-*N,N'*-diacetate

Scott K. Larsen, Bruce G. Jenkins, Nasim G. Memon, and Randall B. Lauffer\*

Received May 1, 1989

Structure-affinity relationships in the binding of iron(III) ethylene-*N,N'*-bis((2-hydroxyphenyl)glycinate) [Fe(EHPG)]<sup>-</sup> diastereomers and iron(III) *N,N'*-bis(2-hydroxybenzyl)ethylenediamine-*N,N'*-diacetate [Fe(HBED)]<sup>-</sup> to human serum albumin (HSA) are elucidated with equilibrium dialysis and water proton NMR relaxation studies. Fe(HBED)<sup>-</sup> and the racemic (*RR* + *SS*) isomer of Fe(EHPG)<sup>-</sup> bind to one apparent site on HSA with association constants on the order of  $(1.1-1.7) \times 10^3 \text{ M}^{-1}$ , whereas the meso (*RS*) isomer of Fe(EHPG)<sup>-</sup> binds only weakly. The relative affinities are apparently a function of phenolate ring orientation: the *cis*-equatorial phenolate coordination exhibited by *rac*-Fe(EHPG)<sup>-</sup> and Fe(HBED)<sup>-</sup> leads to a cylindrical shape that may be more complementary with a cleftlike site on the protein surface than the more distorted *meso*-Fe(EHPG)<sup>-</sup> isomer, which has one axial and one equatorial phenolate. The outer-sphere relaxivities of all three complexes increase by factors of 3-4 upon binding to the protein due to the increased rotational correlation time; this enhancement is consistent with the chelates binding on the protein surface. An X-ray structural analysis was performed on K[Fe(HBED)]·CH<sub>3</sub>OH·CHCl<sub>3</sub>, which crystallizes in the monoclinic *P*2<sub>1</sub>/*a* space group, with *a* = 12.589 (2) Å, *b* = 17.414 (2) Å, *c* = 12.727 (2) Å, β = 102.54°, and *Z* = 4.

### Introduction

The characterization of noncovalent interactions between metal complexes and biological macromolecules is becoming increasingly important as new metal-containing drugs and molecular probes are being developed. For example, *in vivo* binding of paramagnetic complexes used as contrast-enhancing agents in <sup>1</sup>H NMR imaging can alter water relaxation properties as well as the biodistribution of the agents.<sup>1</sup> Secondly, the specificity of DNA-metal complex interactions, which offer new chemical and photochemical tools for molecular biology, is controlled by noncovalent binding.<sup>2</sup> And finally, specific monoclonal antibodies that recognize metal chelates are currently being examined for applications in radioisotope imaging and therapy.<sup>3</sup>

We have been interested in molecular interactions between human serum albumin (HSA) and a series of iron phenolate chelates, which are prototype liver-enhancing agents for NMR imaging.<sup>1,4-7</sup> These chelates include various 5-substituted derivatives of iron(III) ethylene-*N,N'*-bis((2-hydroxyphenyl)glycinate) [Fe(EHPG)]<sup>-</sup> and iron(III) *N,N'*-bis(2-hydroxy-

benzyl)ethylenediamine-*N,N'*-diacetate [Fe(HBED)]<sup>-</sup>, schematic structures for which are shown in Figure 1. Like many hydrophobic drugs and endogenous metabolites, these complexes are transported in the blood bound to HSA. Previous studies have shown that the racemic and meso isomers of Fe(5-Br-EHPG)<sup>-</sup> bind differently to HSA, with the racemic isomer having higher binding affinity and apparent localization into a specific site on the protein that also binds the heme breakdown product, bilirubin-IX<sub>α</sub>.<sup>6</sup> These observations raise the possibility that the three-dimensional shape of the racemic isomer more closely approximates that of bilirubin when bound to HSA. In any event, its shape is certainly important for high binding affinity.

In this work, we extend our studies to the unsubstituted derivatives of Fe(EHPG)<sup>-</sup> and Fe(HBED)<sup>-</sup>. Lacking the hydrophobic bromine substituents, these derivatives possess much lower affinity for HSA; this complicates the analysis of HSA binding affinity by conventional techniques. However we are able to show by both equilibrium dialysis and water <sup>1</sup>H relaxation studies that the preferential binding of the racemic isomer holds for these chelates as well. Moreover, the relatively high binding affinity exhibited by Fe(HBED)<sup>-</sup>, for which our structural analysis reveals a phenolate orientation more closely resembling the racemic isomer, affirms the importance of overall shape in the interactions between HSA and this class of rigid anionic molecules.

### Experimental Section

**Preparation of Complexes.** Fe(EHPG)<sup>-</sup> was prepared by the addition of 1 equiv of EHPG (Sigma) and 1 equiv of NaOH to an aqueous solution of FeCl<sub>3</sub>. After refluxing for 0.5-1.0 h, the solution was evaporated to dryness. The sodium salts of the meso and racemic diastereomers of Fe(EHPG)<sup>-</sup> were isolated by fractional crystallization of the residue in methanol (the meso isomer is first to crystallize) and purified

(1) Lauffer, R. B. *Chem. Rev.* **1987**, *87*, 901-927.

(2) Barton, J. K. *Science* **1986**, *233*, 727-734.

(3) Meares, C. F. *Nucl. Med. Biol.* **1986**, *13*, 319-324.

(4) Lauffer, R. B.; Greif, W. L.; Stark, D. D.; Vincent, A. C.; Wedeen, V. J.; Brady, T. J. *J. Comput. Assist. Tomogr.* **1985**, *9*, 431-438.

(5) Lauffer, R. B.; Vincent, A. C.; Padmanabhan, S.; Villringer, A.; Saini, S.; Elmaleh, D. R.; Brady, T. J. *Magn. Reson. Med.* **1987**, *4*, 582-590.

(6) (a) Lauffer, R. B.; Vincent, A. C.; Padmanabhan, S.; Meade, T. J. *J. Am. Chem. Soc.* **1987**, *109*, 2216-2218. (b) Jenkins, B. G.; Armstrong, E.; Lauffer, R. B. *Magn. Reson. Med.*, in press.

(7) Lauffer, R. B.; Betteridge, D. R.; Padmanabhan, S.; Brady, T. J. *Nucl. Med. Biol.* **1988**, *15*, 45-46.